



# Chemical degradation mechanism of TAPC as hole transport layer in blue phosphorescent OLED



Shou-Cheng Dong<sup>a</sup>, Lisong Xu<sup>b</sup>, Ching W. Tang<sup>a, b, \*</sup>

<sup>a</sup> Department of Chemistry and Institute for Advanced Study, The Hong Kong University of Science and Technology, Hong Kong

<sup>b</sup> Department of Chemical Engineering, University of Rochester, Rochester, NY, 14627, USA

## ARTICLE INFO

### Article history:

Received 11 September 2016

Received in revised form

22 November 2016

Accepted 29 November 2016

Available online 30 November 2016

### Keywords:

LDI-TOF

Laser desorption ionization

OLED

Degradation

## ABSTRACT

The degradation of hole transport materials has been studied via laser desorption ionization-time of flight (LDI-TOF) of aged and unaged OLED devices, TOF/TOF of cations, and DFT calculation of bond dissociation energies. We were able to show that TAPC, one of the archetypal hole-transport materials, undergoes cation induced cyclohexyl ring-opening reaction with device operation. This alternative degradation pathway is in addition to C–N bond dissociation commonly observed in polycyclic aromatic amines.

© 2016 Elsevier B.V. All rights reserved.

## 1. Introduction

1,1-bis((di-4-tolylamino)phenyl)cyclohexane (TAPC) is an archetypal hole-transport material (HTM) used in OLED devices [1]. Its high ionization potential (IP = 5.6 V) and hole mobility ( $\sim 10^{-2} \text{ cm}^2 \text{ V}^{-1} \text{ s}^{-1}$ ) ensure good hole injection and transport. It has a high triplet energy (3.0 eV), which is useful for confining excitons in the emitting layer, particularly in blue phosphorescent and TADF OLEDs. TAPC is still widely used in OLED research, producing some of the highest device efficiencies [2]. However, OLEDs using TAPC showed much shorter lifetime compared to devices using other HTMs, i.e. *N,N'*-Bis-(1-naphthalenyl)-*N,N'*-bis-phenyl-(1,1'-biphenyl)-4,4'-diamine (NPB). Comparing TAPC and NPB based OLED devices [3], Kondakov et al. found that TAPC degrades much faster than NPB and attributed the chemical degradation mainly to C–N bond dissociation. Their analysis indicated that the C–C bond cleavage associated with the cyclohexyl ring also plays a role. In this work, we further studied the chemical degradation of TAPC using laser desorption ionization-time of flight (LDI-TOF) technique [4]. We will show that chemical degradation of TAPC occurs even as

TAPC is isolated from the emitting layer. From molecular fragment structures and theoretically calculated bond dissociation energies, we suggested that cyclohexyl ring-open associated with TAPC cations is a likely pathway for TAPC degradation.

## 2. Experimental

All OLED devices were fabricated on patterned indium-tin-oxide (ITO) (110 nm thickness, 15  $\Omega/\text{sq}$  sheet resistance) coated glass substrates. Prior to film deposition, the substrates were cleaned in deionized water and organic baths with ultra-sonication sequentially, followed by an  $\text{O}_2$  plasma treatment. All films were prepared by vapor deposition at a base pressure of  $10^{-6}$  torr (without breaking vacuum). The deposition rate of each organic layer was monitored by quartz crystal sensors via a side aperture on the boats [5]. To evaluate the device lifetime, all complete OLED devices were transferred to a vacuum assembly after fabrication, with a brief exposure to ambient atmosphere for about 30 s. The devices were then constantly driven at a current density of 5  $\text{mA}/\text{cm}^2$  at room temperature. LDI-TOF and TOF/TOF experiments were performed on Bruker AutoFlex III and Bruker UltrafleXtreme mass spectrometers, respectively. Before loading the samples on a MALDI sample plate, the aluminum cathodes were removed by Kapton tape. The nitrogen laser (337 nm) pulse was set to be 100 Hz. A total of 500 spectra were acquired at each spot position. All data were obtained in positive reflector mode. Gauss09 was used to do density function

\* Corresponding author. Department of Chemistry and Institute for Advanced Study, The Hong Kong University of Science and Technology, Hong Kong; Department of Chemical Engineering, University of Rochester, Rochester, NY, 14627, USA.

E-mail address: [ching.tang@ust.hk](mailto:ching.tang@ust.hk) (C.W. Tang).

theory (DFT) calculations at b3lyp level with 6–31 g(d) as basic set. Sum of electronic and thermal enthalpies were used to estimate bond dissociation energy.

### 3. Results and discussion

We studied TAPC degradation using a blue phosphorescent OLED (Device A) of the following structure: ITO/HATCN (3 nm)/TAPC (40 nm)/TCTA (4 nm)/26DCzPPy:Ir(ipr<sub>3</sub>pmi)<sub>3</sub> (9%, 10 nm)/TmPyPB (10 nm)/TmPyPB:Cs<sub>2</sub>CO<sub>3</sub> (30 nm)/Al. The molecular structure and triplet energy level of materials used are shown in Fig. 1. 1,4,5,8,9,11-hexaazatriphenylene-hexanitrile (HATCN) functions as the hole injection layer and TAPC as the hole transport layer. 4,4,4-tris(*N*-carbazolyl)triphenyl-amine (TCTA) was used as the exciton blocking layer, isolating TAPC from the emitting layer. A bipolar host 2,6-bis(3-(carbazol-9-yl)phenyl)-pyridine (26DCzPPy) [6] was used to sensitize tris[1-(2,6-diisopropylphenyl)-2-phenyl-1H-imidazole] iridium(III) (Ir(ipr<sub>3</sub>pmi)<sub>3</sub>), a relatively stable blue dopant we previously reported [7]. Neat and heavily doped 1,3,5-tri(m-pyrid-3-yl-phenyl)-benzene (TmPyPB) were utilized as the electron transport and electron injection layers, respectively.

Device A exhibited an external quantum efficiency (EQE) over 20% (Fig. 2). Its brightness, starting from 2452 cd/m<sup>2</sup>, dropped below 30% in less than 20 h operation at 5 mA/cm<sup>2</sup>. There was also a steady increase in the drive voltage. This aged device was subjected to LDI-TOF analysis along with an identical but unaged device as reference. Since laser can induce fragmentation of OLED materials, both samples were analyzed in one run at the same laser intensity and mode.

Based on the LDI-TOF and TOF/TOF spectra obtained for each of the materials used in Device A, most of the peaks appeared in Fig. 3 are assigned to proposed molecular structures. Mass peaks at 562, 626, 740 and 1103 correspond to molecular masses of 26DCzPPy, TAPC, TCTA and Ir(ipr<sub>3</sub>pmi)<sub>3</sub>, respectively. HATCN was not detected because of its high IP. TmPyPB was also absent due to its lack of absorption at laser wavelength (337 nm). All the other peaks in the spectra are fragments and adducts, the structures of which are summarized in Table 1.

Since TAPC has lower IP than TCTA and 26DCzPPy, it's dominant peak (626) overshadows other peaks in both aged and unaged samples, except Ir(ipr<sub>3</sub>pmi)<sub>3</sub>, which has the lowest IP in this set of materials. In the aged device, the peaks from TCTA and 26DCzPPy are revealed as the intensity of TAPC fragments is increased, both indicating possible chemical degradation of TAPC. From fragment structures listed in Table 1, two fragmentation pathways can be reconstructed for TAPC: 1) C–N bond cleavage; 2) cyclohexyl rupture. C–N cleavage gives fragments at 431 and 536, and adducts at 717 and 1056. Cyclohexyl rupture results in fragments at 465, 557, 570 and 583. A combination of both yields adduct at 591. Some of these fragments are protonated most likely due to interactions with hydrogen-abundant fragments from cyclohexyl.

In Device A, TAPC is merely used as the hole-transport layer, which is isolated from the EML layer by another hole-transport/exciton confinement layer TCTA. In this structure, excitons formed in EML can hardly affect TAPC layer. For a TAPC molecule to degrade chemically, its cation is implicated. TOF/TOF, a tandem mass technique, provides a useful way to study the intrinsic fragmentation of TAPC cation in vacuum. As shown in Fig. 4, mass peaks

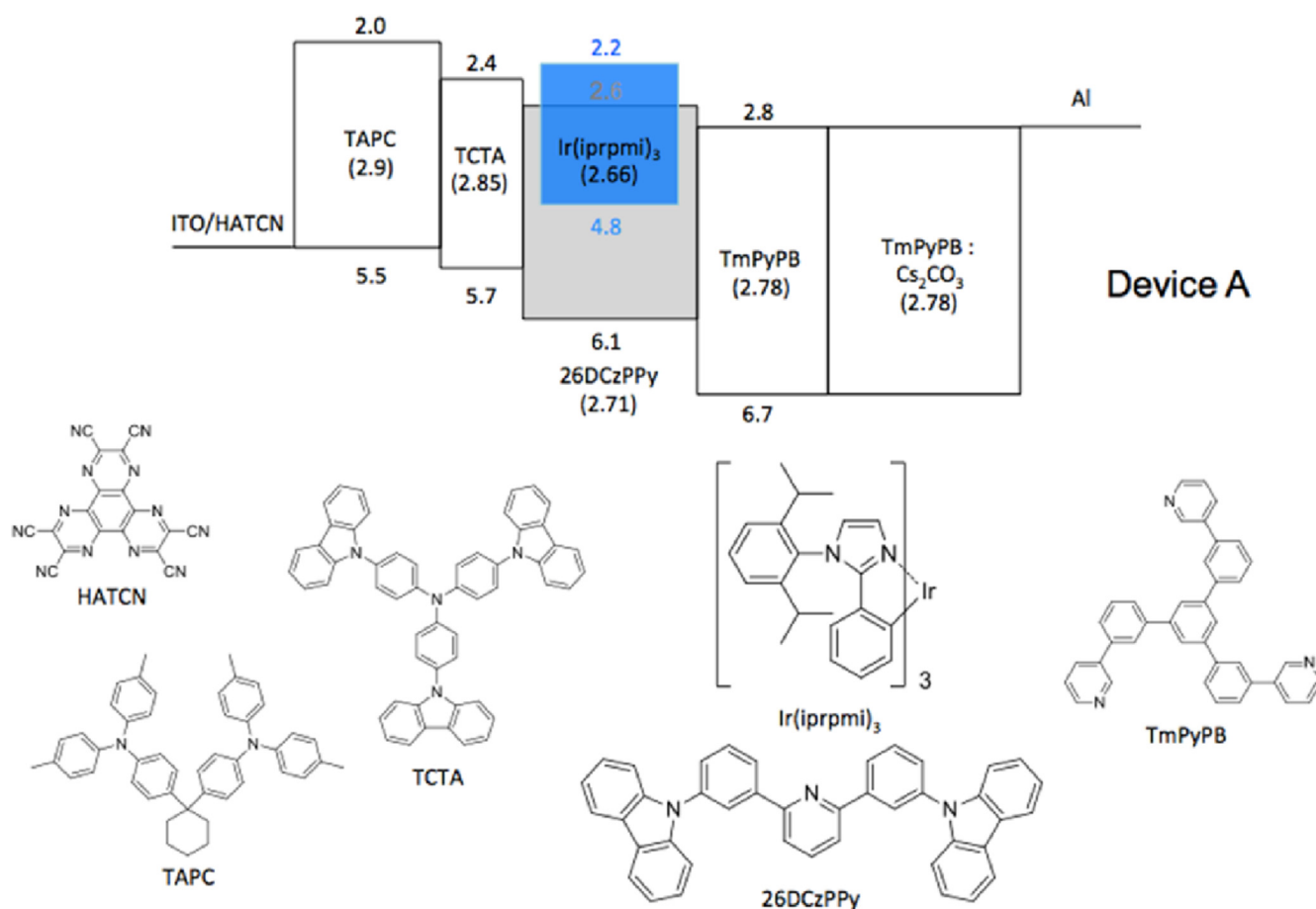


Fig. 1. Energy diagram of Device A and materials used.

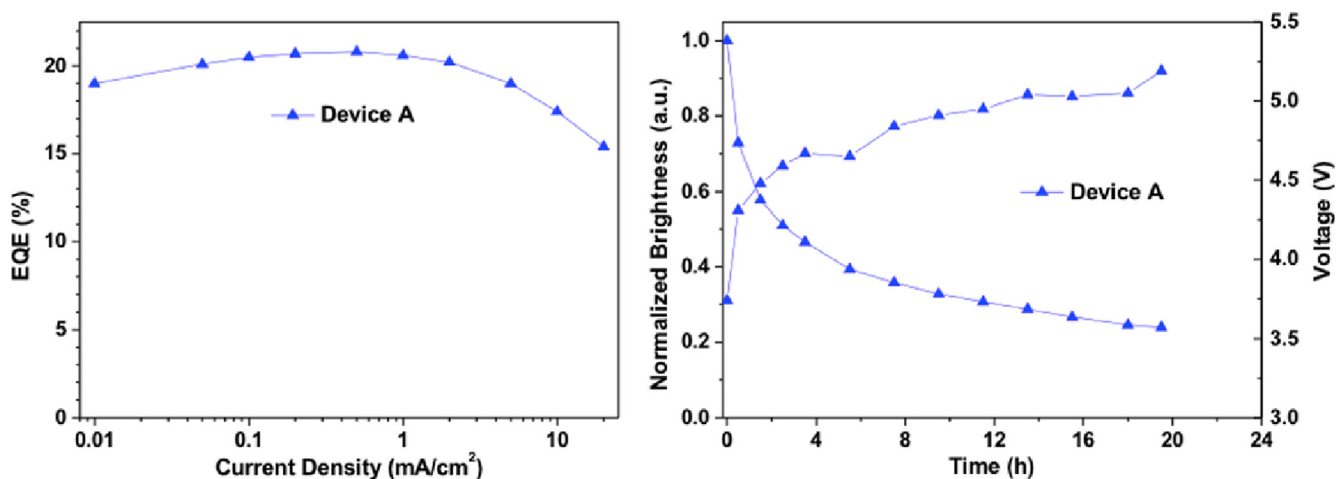


Fig. 2. Efficiency and lifetime performance of Device A.

at 583, which is the product ion of cyclohexyl rupture process, is the dominating fragment in TOF/TOF spectrum of TAPC cation. It strongly suggests that TAPC cation mainly follows a ring rupture chemical degradation pathway rather than the C–N cleavage mechanism [3].

To elucidate the fragmentation of TAPC neutral and TAPC cation in solid films, we compare the LDI-TOF spectra obtained from a neat TAPC film (20 nm) and a HATCN (3 nm)/TAPC (20 nm) bilayer. HATCN, a strong electron acceptor, can produce a TAPC cation in the bilayer by forming a TAPC<sup>+</sup>/HATCN-charge transfer complex. Under low-intensity laser irradiation, the LDI-TOF spectra of these two samples clearly show different fragmentation patterns (Fig. 5). It can be seen that TAPC neutral mainly undergoes C–N cleavage fragmentation, while TAPC cation shows more fragments from cyclohexyl rupture. At higher

laser intensities cyclohexyl rupture fragments can also be found in the neat TAPC film, but the fragment intensity is always much lower than the HATCN/TAPC sample. It can be concluded that direct laser irradiation (337 nm) on neutral TAPC preferentially causes C–N bond dissociation, while irradiation on TAPC cation induces more cyclohexyl ring open reaction. We have observed similar fragmentation patterns of TAPC cations generated by FeCl<sub>3</sub> oxidation.

To explain the different fragmentation of neutral and cationic TAPC, DFT method was utilized to calculate the dissociation energy of each broken bond in both TAPC and TAPC cation (Fig. 6). In neutral TAPC, the dissociation energies of both C–N bonds, which are comparable to the value reported by Kondakov [3], are lower than that of the C–C bond in cyclohexyl ring. However, in a TAPC cation, the C–N bond dissociation energies increase while the

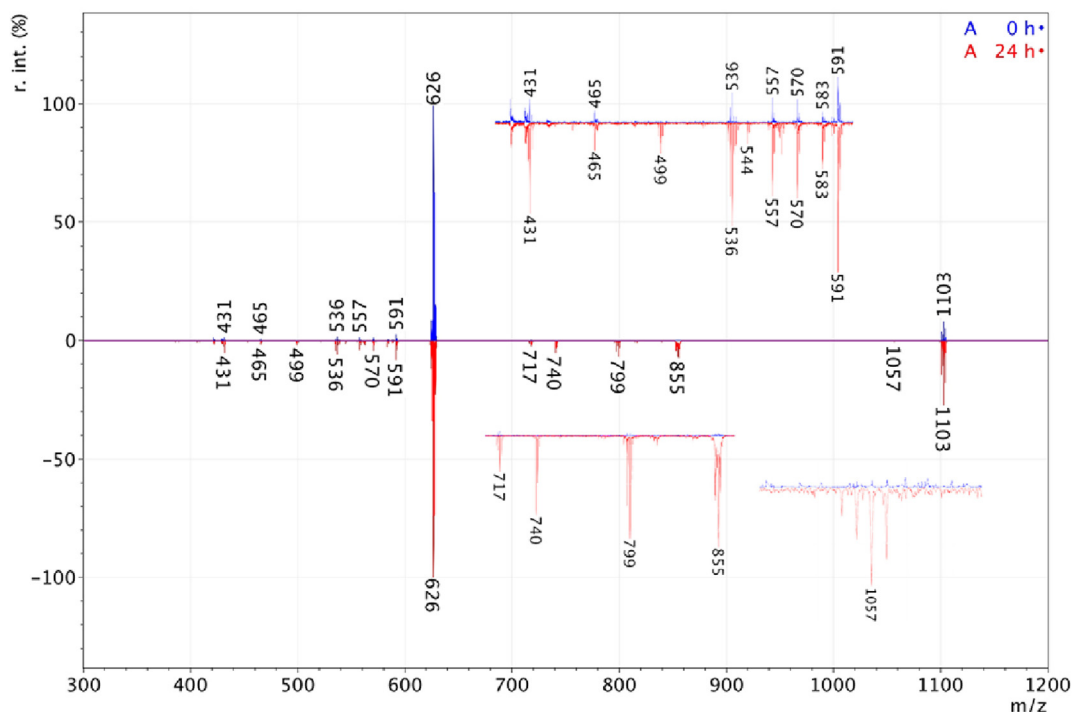


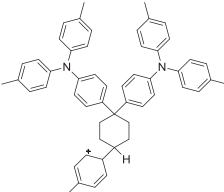
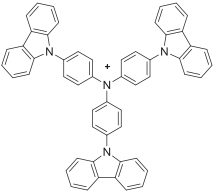
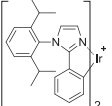
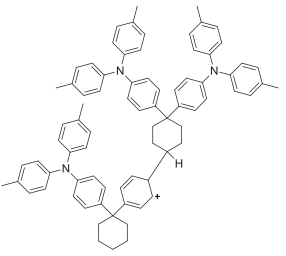
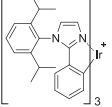
Fig. 3. Normalized LDI-TOF spectra of Device A with and without degradation.

**Table 1**

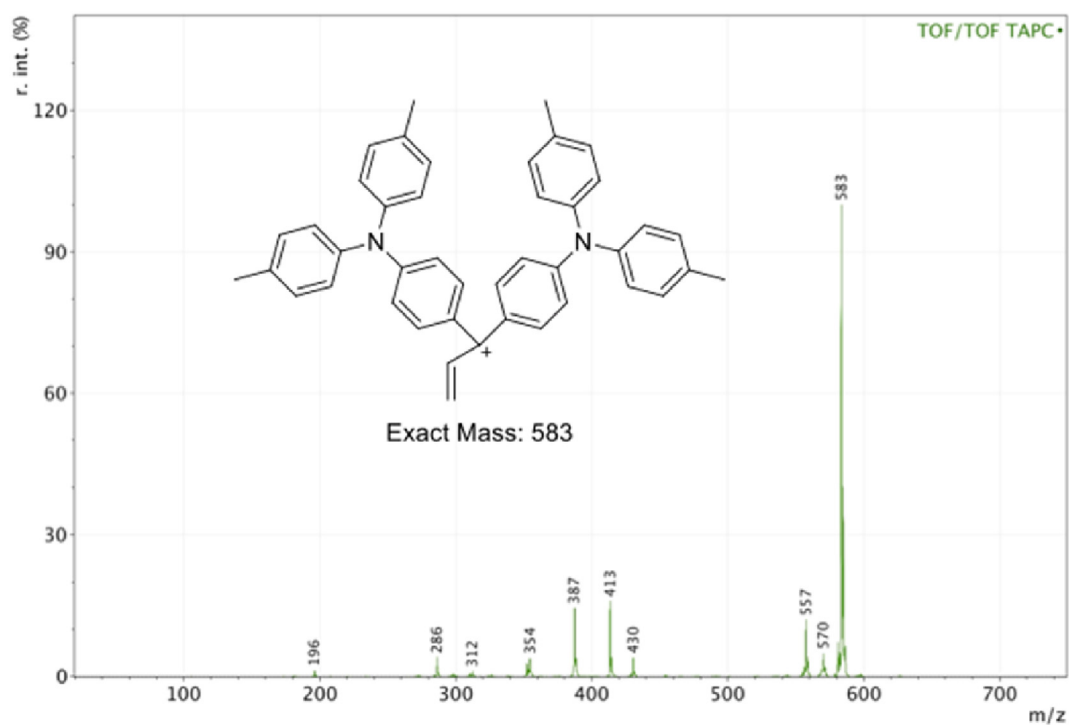
List of mass peaks and their proposed structures.

Mass (m/z)	Origin	Nature	Proposed structure
431	TAPC	Fragment	
465	TAPC	Fragment	
499	TCTA	Fragment	
536	TAPC	Fragment	
557	TAPC	Fragment	
562	26DCzPPy	Molecular mass	
570	TAPC	Fragment	
583	TAPC	Fragment	
591	TAPC	Adduct	
626	TAPC	Molecular mass	

**Table 1** (continued)

Mass (m/z)	Origin	Nature	Proposed structure
717	TAPC	Adduct	
740	TCTA	Molecular mass	
799	Ir(iprpmi) <sub>3</sub>	Fragment	
855 <sup>a</sup>	Ir(iprpmi) <sub>3</sub>	Fragment	Product ion formed by dissociation of meta stable Ir(iprpmi) <sub>3</sub> <sup>+</sup> in post source decay (PSD), possibly has the same structure as 799
1057	TAPC	Adduct	
1103	Ir(iprpmi) <sub>3</sub>	Molecular mass	

<sup>a</sup> Peaks at 855 have abnormally low resolution (large FWHM) and is absent in linear mode, which indicate it is a product ion from precursor dissociation in PSD.


**Fig. 4.** TOF/TOF spectrum of TAPC cation.

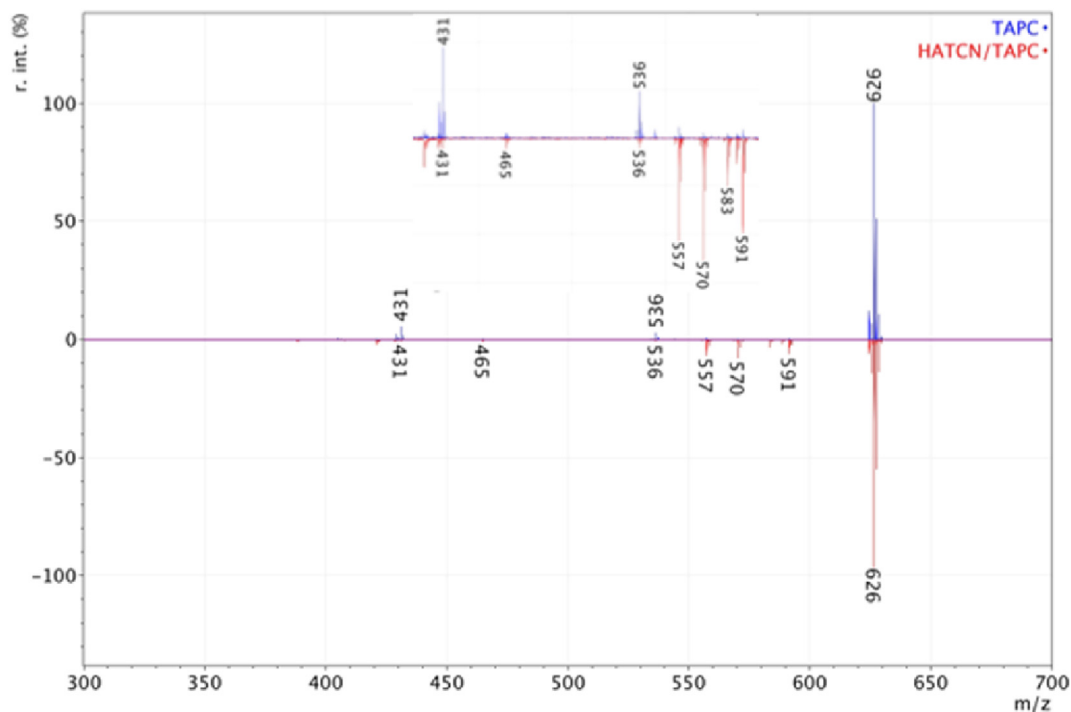


Fig. 5. LDI-TOF spectra of TAPC neat film and HATCN/TAPC bilayer.

cyclohexyl ring open energy drastically decrease to 1.4 eV. Once the cyclohexyl ring is open, further cracking reactions ensue due to the high reactivity of radical cation (Fig. 7). The low energy barrier significantly increases the chance of degradation of TAPC cation, which is in agreement with TOF/TOF and LDI-TOF results.

To understand the origin of low ring open energy in TAPC cation, the resonant forms of TAPC cation and ring-opened TAPC cation, together with calculated HOMOs of TAPC and ring-opened TAPC are illustrated in Fig. 8. In TAPC cation, positive charge is located on either amine group, separated by the center cyclohexyl ring. But

once the ring is open, the central carbon acts like a bridge, delocalizing the positive charge on both amine groups. The extended resonance lowers the energy of reactive radical cation, therefore lowers the energy barrier between TAPC cation and ring-opened TAPC cation. In TAPC, the HOMO is separated by the cyclohexyl ring. While in ring-opened TAPC, HOMO on two amines are connected by the central carbon radical, reasserting the cation induced ring-open mechanism. However, the driving force of this ring opening reaction in OLED device is unclear. It is possible the observed degradation involves excited state TAPC radical cations, which may be produced via photo-excitation from light emitted by the device.

Fragmentations of TCTA and the dopant Ir(ppy)<sub>3</sub> were observed in degraded sample at 499 and 799. However, it is hard to draw any conclusion about the origin of these fragmentations due to matrix effect and IP hierarchy of analytes [8]. The peak intensity may not necessarily reflect actual abundance of each species. As mentioned, LDI-TOF signals from TAPC and its fragments can overshadow other peaks, making it hard to analyze possible

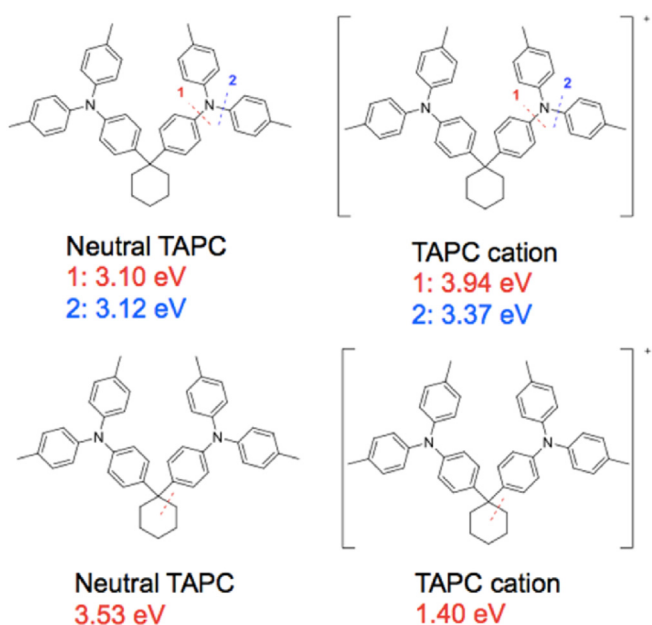


Fig. 6. Dissociation energy of bonds in TAPC and TAPC cation.

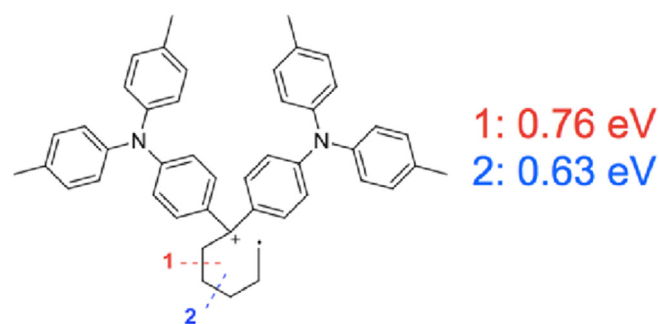


Fig. 7. Dissociation energy of cracking reactions after cyclohexyl is opened in TAPC cation. Dissociation of 1 corresponds to fragments at 570 and 591 and 2 corresponds to peaks at 583.



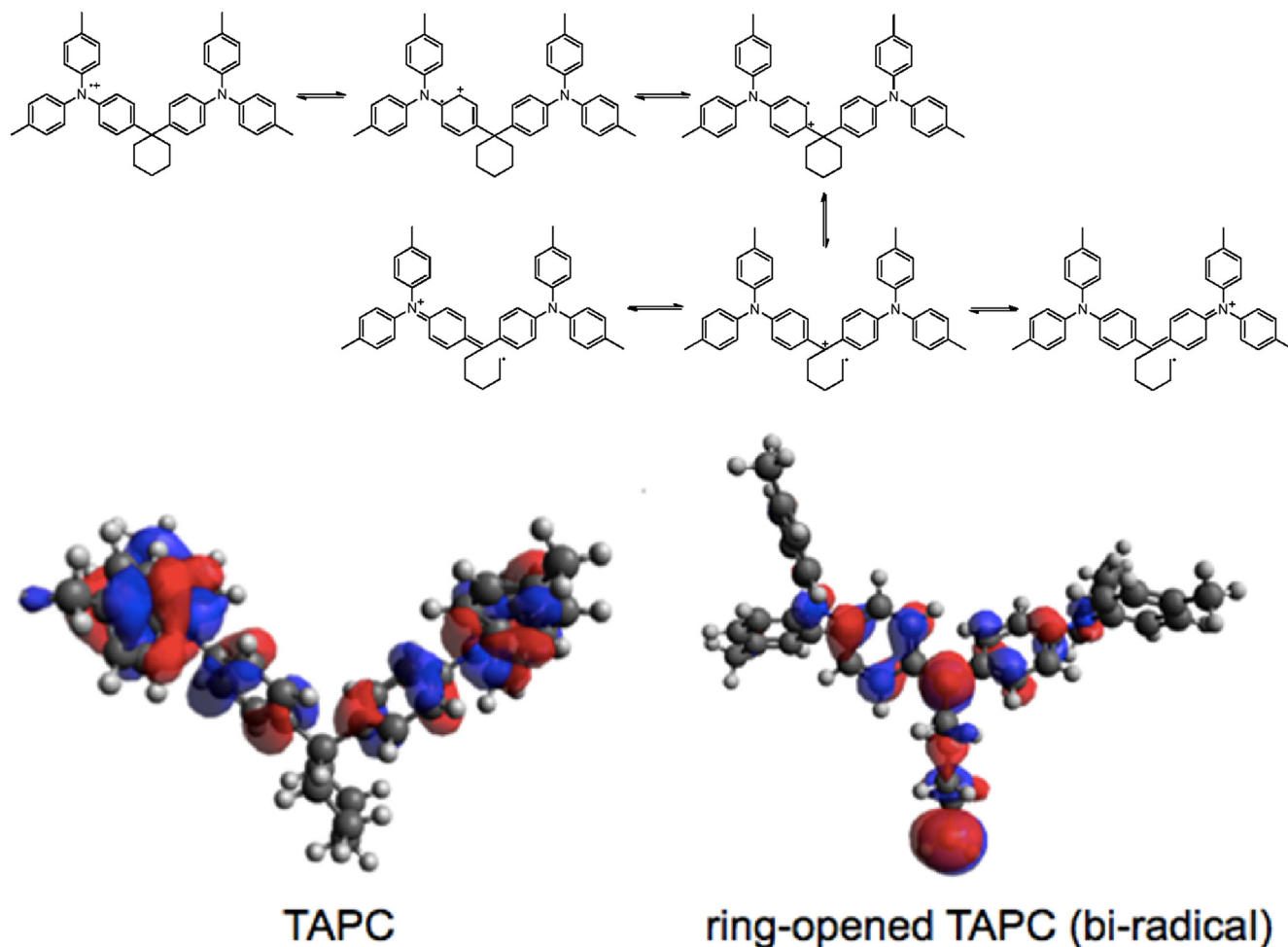


Fig. 8. Resonant structures (up) of TAPC cation and ring-opened TAPC cation and HOMO (down) of TAPC and ring-opened TAPC.

degradation of other materials such as TCTA in the presence of TAPC.

LDI involves complex chemistry processes, including intramolecular fragmentation, intermolecular energy and electron transfer, and reactions between active species [9–11]. The significant increase of TAPC fragments observed in degraded sample may only account for the presence of minute amount of degraded species in the TAPC layer. In situ LDI-TOF on a complex cell such as Device A may only be suitable for the analysis of less stable materials such as Flrpic [12] and/or severely degraded devices [13].

#### 4. Conclusion

In conclusion, we have established a methodology to study the degradation of hole transport materials via LDI-TOF of aged and unaged devices, TOF/TOF of cations, and DFT calculated bond dissociation energies. We were able to show that TAPC as a hole-transport molecule undergoes cation induced cyclohexyl ring-opening reaction as a likely degradation pathway. This finding suggests that TAPC is not a robust hole-transport material for OLED devices due to the intrinsic instability of its radical cation.

#### Author contributions

L. Xu fabricated OLED devices and conducted LDI-TOF experiments. S.-C. Dong performed TOF/TOF experiment and DFT

calculation, and prepared the manuscript. C. W. Tang supervised the research and revised the manuscript.

#### Acknowledgements

This work was supported by IAS at HKUST. The authors would like to thank Ms Pui Shuen (Joyce) Wong at BioCRF, HKUST for her assistance in LDI-TOF and TOF/TOF analysis.

#### References

- [1] C.W. Tang, S.A. VanSlyke, Organic electroluminescent diodes, *Appl. Phys. Lett.* 51 (1987) 913.
- [2] L.-S. Cui, J.U. Kim, H. Nomura, H. Nakanotani, C. Adachi, Benzimidazobenzothiazole-based bipolar hosts to harvest nearly all of the excitons from blue delayed fluorescence and phosphorescent organic light-emitting diodes, *Angew. Chem. Int. Ed.* 55 (2016) 6864.
- [3] D.Y. Kondakov, Role of chemical reactions of arylamine hole transport materials in operational degradation of organic light-emitting diodes, *J. Appl. Phys.* 104 (2008) 084520.
- [4] S. Scholz, K. Walzer, K. Leo, Analysis of complete organic semiconductor devices by laser desorption/ionization time-of-flight mass spectrometry, *Adv. Funct. Mater.* 18 (2008) 2541.
- [5] L. Xu, C.W. Tang, L.J. Rothberg, High efficiency phosphorescent white organic light-emitting diodes with an ultra-thin red and green co-doped layer and dual blue emitting layers, *Org. Electron.* 32 (2016) 54–58.
- [6] S.-J. Su, C. Cai, J. Kido, RGB phosphorescent organic light-emitting diodes by using host materials with heterocyclic cores: effect of nitrogen atom orientations, *Chem. Mater.* 23 (2011) 274.
- [7] K.P. Klubek, S.-C. Dong, L.-S. Liao, C.W. Tang, L.J. Rothberg, Investigating blue phosphorescent iridium cyclometalated dopant with phenyl-imidazole

- ligands, *Org. Electron* 15 (2014) 3127.
- [8] A.J. Hotelling, W.F. Nichols, D.J. Giesen, J.R. Lenhard, R. Knochenmuss, Electron transfer reactions in LDI and MALDI: factors influencing matrix and analyte ion intensities, *Eur. J. Mass Spectrom.* 12 (2006) 345.
- [9] M. Karas, R. Krüger, Ion formation in MALDI: the cluster ionization mechanism, *Chem. Rev.* 103 (2003) 427.
- [10] K. Dreisewerd, The desorption process in MALDI, *Chem. Rev.* 103 (2003) 395.
- [11] R. Knochenmuss, R. Zenobi, MALDI ionization: the role of in-plume processes, *Chem. Rev.* 103 (2003) 441.
- [12] R. Seifert, I.R. de Moraes, S. Scholz, M.C. Gather, B. Lüssem, K. Leo, Chemical degradation mechanisms of highly efficient blue phosphorescent emitters used for organic light emitting diodes, *Org. Electron* 14 (2013) 115.
- [13] I.R. de Moraes, S. Scholz, B. Lüssem, K. Leo, Chemical degradation processes of highly stable red phosphorescent organic light emitting diodes, *Org. Electron* 13 (2012) 1900.